



**HAL**  
open science

## Role of isospin in the nuclear liquid-gas phase transition

F. Gulminelli, C. Ducoin, P. Dr Chomaz

► **To cite this version:**

F. Gulminelli, C. Ducoin, P. Dr Chomaz. Role of isospin in the nuclear liquid-gas phase transition. 2005. in2p3-00025179v1

**HAL Id: in2p3-00025179**

**<https://hal.in2p3.fr/in2p3-00025179v1>**

Preprint submitted on 6 Dec 2005 (v1), last revised 16 Mar 2006 (v2)

**HAL** is a multi-disciplinary open access archive for the deposit and dissemination of scientific research documents, whether they are published or not. The documents may come from teaching and research institutions in France or abroad, or from public or private research centers.

L'archive ouverte pluridisciplinaire **HAL**, est destinée au dépôt et à la diffusion de documents scientifiques de niveau recherche, publiés ou non, émanant des établissements d'enseignement et de recherche français ou étrangers, des laboratoires publics ou privés.

# Role of isospin in the nuclear liquid-gas phase transition

C. Ducoin<sup>(1,2)</sup>, Ph. Chomaz<sup>(1)</sup> and F. Gulminelli<sup>(2)</sup>

(1) GANIL (DSM-CEA/IN2P3-CNRS), B.P.5027, F-14076 Caen cédex 5, France

(2) LPC (IN2P3-CNRS/Ensicaen et Université), F-14050 Caen cédex, France

We study the thermodynamics of asymmetric nuclear matter using a mean field approximation with a Skyrme effective interaction, in order to establish its phase diagram and more particularly the influence of isospin on the order of the transition. A new statistical method is introduced to study the thermodynamics of a multifluid system, keeping only one density fixed the others being replaced by their intensive conjugated variables. In this ensemble phase coexistence reduces to a simple one dimensional Maxwell construction. For a fixed temperature under a critical value, a coexistence line is obtained in the plane of neutron and proton chemical potentials. Along this line the grand potential presents a discontinuous slope showing that the transition is first order except at the two ending points where it becomes second order. This result is not in contradiction with the already reported occurrence of a continuous transformation when a constant proton fraction is imposed. Indeed, the proton fraction being an order parameter in asymmetric matter, the constraint can only be fulfilled by gradual phase mixing along the first-order phase transition line leading to a continuous pressure.

PACS numbers: 24.10.Pa,64.60.Fr,68.35.Rh

## I. INTRODUCTION

Nucleons in atomic nuclei interact through a finite-range attractive and a short-range repulsive force. For systems of particles interacting this way, one expects to find a phase transition analogous to the liquid-gas transition of a Van der Waals fluid [1]. As a matter of fact, it is recognized that symmetric nuclear matter should undergo a first order transition between a low (gas) and a high (liquid) density phase up to a critical temperature [2, 3, 4]. For such a system containing an equal number of neutrons and protons, the isospin symmetry imposes that the nucleons behave as one single fluid and one expects a discontinuous density versus pressure equation of state.

The case of asymmetric matter is more complex to study, since there is an additional degree of freedom to consider: the isospin. Such matter plays an important role in astrophysics where neutron rich systems are involved in neutron stars and type-II supernova evolutions [5, 6]. For asymmetric systems containing a fixed proton fraction, it has been shown that the thermodynamic transformations result in a continuous evolution of the observables. In particular, the system density is a continuous function of the pressure. This has been interpreted as the occurrence of a continuous transition [7, 8, 9, 10, 11, 12]. We will show in the present article that this conclusion is not correct: it results from a confusion between the notions of 'continuous transition' and 'continuous transformation'. Indeed, the phenomenon of isospin distillation demonstrates that the proton fraction is an order parameter in asymmetric nuclear matter. Thus, when the proton fraction is kept constant, the system is forced to follow the first order phase transition line, hiding the discontinuity of the thermodynamic potential first derivative.

The plan of the paper is as follows: after a short defi-

nition of phase transitions and their order, we calculate in Section III the nuclear-matter grand potential in the mean-field approximation using a Skyrme Sly230a energy density functional [13]. The thermodynamics of nuclear matter has been addressed earlier with different effective forces [15, 16, 17, 18]. In section IV, the mean-field instabilities are corrected introducing phase separation with the construction of a concave envelope for the thermodynamic potential. To perform this Gibbs construction with an arbitrary number of conserved quantities, we introduce a new method that reduces this multidimensional problem to a simple one-dimensional Maxwell construction on a carefully defined statistical potential. The result of this analysis is that the grand-canonical potential presents a discontinuous derivative on both sides of a bi-dimensional manifold limited by a critical line in the 3-dimensional space including the temperature and the proton and neutron chemical potentials. The transition is thus first order for all associated proton fractions. Only the critical line corresponds to continuous transitions. An interesting point is that in this 3-dimensional problem the critical line can be characterized by additional critical exponents as the chemical potential approaches its critical value for a given temperature. The thermodynamic consequences of a transformation at constant proton fraction are analyzed in Sections V and VI. We show that this transformation forces the system to follow the coexistence line, and this is the generic behavior expected when a conservation law acts on an order parameter. Then, the first order phase transition results in a continuous transformation from a diluted to a dense system through a phase coexistence, which should not be confused with a continuous transition.

## II. GENERALITIES ON PHASE TRANSITIONS

For systems at the thermodynamic limit, the existence and the order of a phase transition are intrinsically related to the singularities of the thermodynamic potential,  $-T \ln Z(\lambda)$  where  $Z(\lambda)$  is the partition sum for a given macroscopic state characterized by the  $L$  intensive parameters  $\lambda = \{\lambda_\ell\}$  [14]. These intensive parameters are the Lagrange multipliers introduced in the maximization of the Shannon entropy under the  $L$  constraints  $\langle \hat{A}_\ell \rangle$  associated with all the  $L$  relevant observables  $\hat{A}_\ell$ .

A system presents a first-order phase transition if one of the first partial-derivatives of  $\ln Z(\lambda)$  shows a discontinuity [1]. If a non-analyticity (discontinuity or divergence) is present at a higher order derivative, there is a continuous transition. Since the equations of states (EOS) are the  $L$  relations  $\langle \hat{A}_\ell \rangle(\lambda) = -\partial_{\lambda_\ell} \ln Z(\lambda)$  [14], we can see that a first-order phase transition corresponds to a discontinuity in at least one of the EOS, i.e. to a jump in the mean value of at least one observable at the transition point. This observable can then be identified with an order parameter since its value allows to distinguish the two coexisting phases.

### III. SKYRME GRAND POTENTIAL

#### A. Isospin dependent energy functional

We study the case of nuclear matter in a mean field approach, with the SLy230a Skyrme effective interaction [13]. This local interaction allows to introduce an energy density hamiltonian  $\mathcal{H}(\mathbf{r})$  so that the total energy for a system of nucleons in a Slater determinant  $|\psi\rangle$  reads :

$$\langle \psi | \hat{H} | \psi \rangle = \int \mathcal{H}(\mathbf{r}) d\mathbf{r}$$

The energy density  $\mathcal{H}$  is a functional of the particle densities  $\rho_q$  and kinetic densities  $\tau_q$  for neutrons ( $q = n$ ) and protons ( $q = p$ ). Noting  $\hat{\rho}_q$  the one-body density matrix of the particles of type  $q$ , those quantities are expressed as follows:  $\rho_q(r) = \langle r | \hat{\rho}_q | r \rangle$  and  $\tau_q(r) = \langle r | \frac{1}{\hbar^2} \hat{p} \hat{\rho}_q \hat{p} | r \rangle$ , such that  $\frac{\hbar^2}{2m} \tau_q$  is the kinetic energy density.

For later convenience it is useful to introduce the isoscalar and isovector densities :

$$\begin{aligned} \rho &= \rho_n + \rho_p, & \tau &= \tau_n + \tau_p \\ \rho_3 &= \rho_n - \rho_p, & \tau_3 &= \tau_n - \tau_p \end{aligned}$$

In the case of homogeneous, spin-saturated matter with no coulomb interaction, four terms contribute to the energy density :

$$\mathcal{H} = \mathcal{K} + \mathcal{H}_0 + \mathcal{H}_3 + \mathcal{H}_{eff}$$

In this expression,  $\mathcal{K}$  is the kinetic-energy term,  $\mathcal{H}_0$  a density-independent two-body term,  $\mathcal{H}_3$  a density-

dependent term, and  $\mathcal{H}_{eff}$  a momentum-dependent term:

$$\begin{aligned} \mathcal{K} &= \frac{\hbar^2}{2m} \tau \\ \mathcal{H}_0 &= C_0 \rho^2 + D_0 \rho_3^2 \\ \mathcal{H}_3 &= C_3 \rho^{\sigma+2} + D_3 \rho^\sigma \rho_3^2 \\ \mathcal{H}_{eff} &= C_{eff} \rho \tau + D_{eff} \rho_3 \tau_3 \end{aligned}$$

The coefficients  $C_i$  and  $D_i$ , associated respectively with the symmetry and asymmetry contributions, are linear combinations of the traditional Skyrme parameters :

$$\begin{aligned} C_0 &= 3t_0/8 \\ D_0 &= -t_0(2x_0 + 1)/8 \\ C_3 &= t_3/16 \\ D_3 &= -t_3(2x_3 + 1)/48 \\ C_{eff} &= [3t_1 + t_2(4x_2 + 5)]/16 \\ D_{eff} &= [t_2(2x_2 + 1) - t_1(2x_1 + 1)]/16 \end{aligned}$$

To illustrate the SLy energy functional we present in Figure 1 the energy density and the energy per particle as a function of the total particle density for various proton fractions. The kinetic-energy term has been computed integrating over the Fermi spheres associated with the considered proton and neutron densities. The minimum of the energy per particle is the saturation point of symmetric matter  $\rho_0 = 0.16 \text{ fm}^{-3}$  and  $E_0 = -15.99 \text{ MeV}$ , while the curvature gives the incompressibility  $K = 230.9 \text{ MeV}$ . The  $Z/A = 0$  curves correspond to pure neutron matter which does not saturate, the Sly forces being fitted on realistic neutron-matter EOS calculations [13, 18].

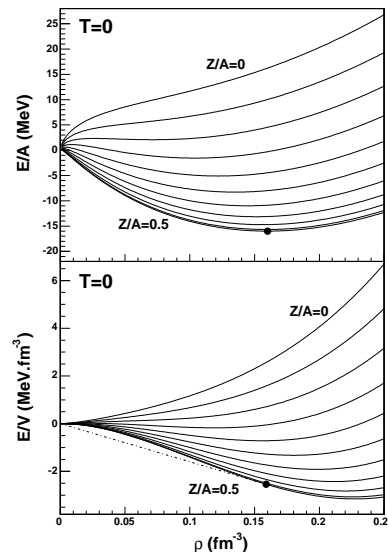


FIG. 1: Sly230a functional for infinite nuclear matter : energy per particle (upper part) and energy density (lower part) as functions of the total nucleon density for regularly spaced proton fractions from  $Z/A=0.5$  to  $Z/A=0$ .

## B. Mean-field Hamiltonian

The mean-field effective hamiltonian  $\hat{W}_q$  for each particle-type  $q$  is defined by the relation  $\delta\langle\hat{H}\rangle = Tr(\hat{W}_q\delta\rho_q)$  i.e. as a functional derivative of the energy density. In the Skyrme case this leads to the expression :

$$\hat{W}_q = \frac{\partial\mathcal{H}}{\partial\tau_q} \frac{\hat{p}^2}{\hbar^2} + \frac{\partial\mathcal{H}}{\partial\rho_q} = \frac{1}{2m_q^*} \hat{p}^2 + U_q$$

where  $U_q = \partial_{\rho_q}\mathcal{H}$  is the local mean-field potential :

$$\begin{aligned} U_q &= U_{0_q} + U_{3_q} + U_{eff_q} \\ &= 1/2[2C_0\rho + (\sigma + 2)C_3\rho^{\sigma+1} + \sigma D_3\rho^{\sigma-1}\rho_3^2 + C_{eff}\tau] \\ &\quad \pm 1/2[2D_0\rho_3 + 2D_3\rho^\sigma\rho_3 + D_{eff}\tau_3] \end{aligned} \quad (1)$$

and the effective mass  $m_q^*$  is defined by :

$$\frac{\hbar}{2m_q^*} = 1/2\left[\frac{\hbar}{2m} + C_{eff}\rho \pm D_{eff}\rho_3\right] \quad (2)$$

In both expression, the  $\pm$  sign refers to neutrons (+) or protons (-).

In uniform nuclear matter, the eigenstates of this mean-field hamiltonian are spin-up or spin-down plane waves with usual quantification relations on their momenta  $\mathbf{p}_i$ . The single-particle energies are given by :

$$\epsilon_q^i = \frac{p_i^2}{2m_q^*} + U_q$$

## C. Finite temperature

Within a mean-field approach thermodynamic relations are easy to derive in the grand-canonical ensemble. For a system of neutrons and protons, the grand-canonical constraint imposes the average value of three observables: energy, number of protons and neutrons. Maximizing the Shannon entropy with these three constraints leads to an equilibrium partition sum :

$$Z_{GC} = Tr[e^{-\beta\hat{H} + \alpha_n\hat{N}_n + \alpha_p\hat{N}_p}]$$

where the inverse temperature  $\beta = 1/kT$  is the Lagrange multiplier associated with the energy constraint, and  $\alpha_q = \beta\mu_q$  are the Lagrange multipliers controlling the particle numbers  $\langle\hat{N}_q\rangle$ ,  $\mu_q$  being the chemical potentials. The Lagrange parameters fulfill the equations of state :

$$\langle\hat{H}\rangle = -\partial_\beta \ln Z_{GC} \quad (3)$$

$$\langle\hat{N}_q\rangle = \partial_{\alpha_q} \ln Z_{GC} \quad (4)$$

The self-consistent mean-field approximation amounts to use independent particle states as trial density matrices in the maximum entropy variational principle: the

single-particle states of energy  $\epsilon_q^i$  are then occupied according to the Fermi-Dirac distribution [19] :

$$n_q^i = \frac{1}{1 + \exp(\beta(\epsilon_q^i - \mu_q))}$$

In infinite matter,  $n_q^i$  is a continuous distribution  $n_q(p)$  and the densities  $\rho_q$  and  $\tau_q$  read :

$$\rho_q = 2 \int_0^\infty n_q(p) \frac{4\pi p^2}{h^3} dp \quad (5)$$

$$\tau_q = 2 \int_0^\infty \frac{p^2}{\hbar^2} n_q(p) \frac{4\pi p^2}{h^3} dp \quad (6)$$

where the factor 2 come from the spin degeneracy.

The first equation establishes a self-consistent relation between the density of  $q$ -particles  $\rho_q$  and their chemical potential  $\mu_q$ . The above densities can be written as regular Fermi integrals by shifting the chemical potential according to  $\mu'_q = \mu_q - U_q$ . The Fermi-Dirac distribution indeed reads :

$$n_q(p) = \frac{1}{1 + \exp(\beta(p^2/2m_q^* - \mu'_q))} \quad (7)$$

Equations (7) and (5) define a self-consistent problem since  $m_q^*$  depends on the densities according to eq.(2). For each couple  $(\mu'_n, \mu'_p)$  a unique solution  $(\rho_n, \rho_p)$  is found by iteratively solving the self-consistency between  $\rho_{n,p}$  and  $m_{n,p}^*$ . Then eq.(6) is used to calculate  $\tau_{n,p}$ . These quantities allow to compute the one-body partition sum :

$$Z_0 = Tr[e^{-\beta(\hat{W}_n + \hat{W}_p - \mu_n\hat{N}_n - \mu_p\hat{N}_p)}] = Z_0^n Z_0^p$$

where each partition sum  $Z_0^q$  can be expressed as a function of the corresponding kinetic energy density :

$$\frac{\ln Z_0^q}{V} = 2 \int_0^\infty \ln(1 + e^{-\beta(\frac{p^2}{2m_q^*} - \mu'_q)}) \frac{4\pi p^2}{h^3} dp = \frac{\hbar^2}{3m_q^*} \beta \tau_q$$

At the thermodynamic limit the system volume  $V$  diverges together with the particle numbers  $\langle\hat{N}_q\rangle$ , and the thermodynamics is completely defined as a function of the two particle densities  $\rho_n, \rho_p$ .

## D. Grand potential

We can now use the maximum-entropy variational principle to evaluate the mean-field approximation to the grand-canonical partition sum  $Z_{GC}$ . We recall that the exact grand-canonical ensemble corresponds to the maximum of the constrained Shannon entropy which is nothing but  $\ln Z_{GC}$  :

$$\ln Z_{GC} = S_{GC} - \beta(\langle\hat{H}\rangle_{GC} - \mu_n\langle\hat{N}_n\rangle_{GC} - \mu_p\langle\hat{N}_p\rangle_{GC}).$$

The variational principle thus states that the mean-field constrained entropy is the best approximation

within the ensemble of independent-particle trial states to the exact maximum  $\ln Z_{GC}$ :

$$\ln Z_{GC} \simeq S_0 - \beta(\langle \hat{H} \rangle_0 - \mu_n \langle \hat{N}_n \rangle_0 - \mu_p \langle \hat{N}_p \rangle_0),$$

where the mean-field energy and particle numbers are defined as functions of densities, i.e. single-particle occupations eq.(7), by :

$$\langle \hat{H} \rangle_0 = V\mathcal{H}; \quad \langle \hat{N}_q \rangle_0 = V\rho_q$$

The mean-field entropy is given by :

$$S_0 = \ln Z_0 + \beta(\langle \hat{W} \rangle_0 - \mu_n \langle \hat{N} \rangle_0 - \mu_p \langle \hat{N}_p \rangle_0)$$

where  $\langle \hat{W} \rangle_0$  represents the average single particle energy :

$$\langle \hat{W} \rangle_0 = 2V \sum_q \int_0^\infty n_q(p) e_q(p) \frac{4\pi p^2}{h^3} dp = -\partial_\beta \ln Z_0$$

with  $e_q(p) = p^2/2m_q^* + U_q$ .

The grand-canonical partition sum in the mean-field approximation is thus modified with respect to the independent-particle partition sum  $Z_0$  as :

$$\ln Z_{GC} \simeq \ln Z_0 + \beta \left( \langle \hat{W} \rangle_0 - \langle \hat{H} \rangle_0 \right)$$

which allows to express the grand-canonical potential density as a function of densities :

$$-g = \frac{\ln Z_{GC}}{\beta V} \simeq \frac{2}{3}\mathcal{K} + \mathcal{H}_0 + (\sigma + 1)\mathcal{H}_3 + \frac{5}{3}\mathcal{H}_{eff}$$

At the thermodynamic limit, this quantity is equivalent to the system pressure  $P = -g$ . Because of ensemble equivalence we can then evaluate all the thermodynamic potentials. For example, the canonical partition sum or equivalently the free energy per unit volume is defined through the Legendre transform :

$$f = -\frac{\ln Z_C}{\beta V} = g + \mu_n \rho_n + \mu_p \rho_p$$

### E. Skyrme grand potential and phase transition

Figure 2 presents the pressure as a function of the isoscalar and isovector chemical potentials  $\mu = \mu_n + \mu_p$  and  $\mu_3 = \mu_n - \mu_p$ . This figure is computed for a uniform system at a fixed temperature  $T = 6MeV$ . For symmetry reasons only the positive  $\mu_3$  are shown. We can see that for some values of  $(\mu, \mu_3)$ , there are three solutions corresponding to different values for the conjugated observables  $(\rho, \rho_3)$ . This is the phase transition region. The true equilibrium is the solution minimizing the grand potential i.e. maximizing the pressure. Thus only the upper part of the pressure manifold corresponds to a thermodynamic equilibrium. At the resulting fold the slope changes discontinuously, i.e. using  $\rho_q = \partial g / \partial \mu$ , the equilibrium uniform system jumps from a low to a high density solution. It is a liquid-gas first-order phase transition.

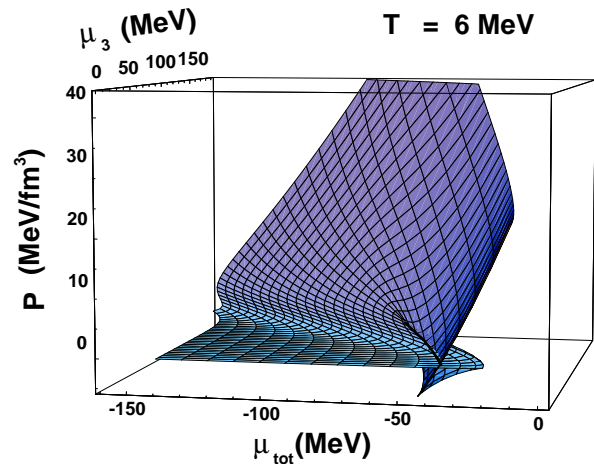


FIG. 2: Pressure as a function of the isoscalar and isovector chemical potentials for a uniform system at  $T = 6MeV$ .

## IV. GIBBS CONSTRUCTION

### A. Phase coexistence conditions in multi-fluid systems

At the thermodynamic limit, the entropy  $S$ , as all the extensive variables  $\{A_k\}$ , is additive and thus scales like the volume  $V$  :

$$S(V, \{A_k\}) = Vs(\rho_k = \{A_k/V\})$$

The volume can thus be eliminated from the thermodynamic description while the other extensive variables can be expressed as densities  $\rho = \{\rho_k\}$ . If we consider two isolated systems of volume  $V_1 = \alpha V$  and  $V_2 = (1 - \alpha)V$ , their constrained entropy is simply the sum of the two entropies  $S = S_1 + S_2$ . When 1 and 2 are put into contact to form a system with  $\rho = \alpha\rho_1 + (1 - \alpha)\rho_2$ , equilibrium is reached by maximization of the global entropy  $S$  so that :

$$S \geq S_1 + S_2 .$$

This imposes the convexity of the entropy :

$$s(\alpha\rho_1 + (1 - \alpha)\rho_2) \geq \alpha s(\rho_1) + (1 - \alpha)s(\rho_2)$$

As a result, if the homogeneous system has a constrained entropy with a convex region, a linear interpolation between two densities  $\rho_A$  and  $\rho_B$  corresponds to a physical phase mixing of the two associated states and leads to a concave envelope which maximizes the entropy functional (Gibbs construction). The straight lines corresponding to phase coexistence are defined by two points of same tangent plane i.e. with identical first derivatives or intensive variables,  $\lambda_k = \partial_{\rho_k} s$ , and equal values of the constrained entropy, i.e. equal distance between the entropy  $s(\rho)$  and the plane  $\sum_k \lambda_k \rho_k = 0$ . Using  $\partial_V S(V, \{A_k\}) = s(\{\rho_k\}) - \sum_k \lambda_k \rho_k$  this latter condition

can be interpreted as the equality of the two system pressures. This equality of all intensive variables defines the conditions of phase equilibrium.

### B. Canonical ensemble

For nuclear matter at a given temperature, the  $A_k$  are the proton and neutron numbers:  $N = \rho_n V$  and  $Z = \rho_p V$ . Finding two points in equilibrium means finding two sets of densities  $\{\rho_n^A, \rho_p^A\}$  and  $\{\rho_n^B, \rho_p^B\}$  which fulfill the 3 equations  $\mu_n^A = \mu_n^B$ ,  $\mu_p^A = \mu_p^B$ ,  $P^A = P^B$ , the equality of the temperatures being insured by the use of an isothermal ensemble. The path corresponding to a constant  $\mu_q$  (e.g.  $\mu_n$ ) is a curve in the  $(\mu_p, P)$  plane that can be determined numerically. The problem is now reduced to two dimensions: if this path shows a crossing point, there are two sets of extensive observables for which the intensive parameters are all equal, which is the condition for coexistence.

This is illustrated in the central part of Fig.3. This is a systematic way to look for phase coexistence in a multi-component system.

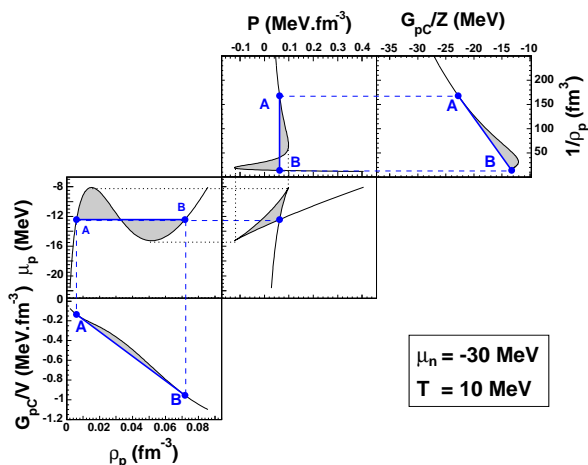


FIG. 3: Illustration of a Maxwell-Gibbs construction in the proton-canonical and neutron grand-canonical ensemble at a fixed neutron chemical potential  $\mu_n = -30 \text{ MeV}$  and temperature  $T = 10 \text{ MeV}$ . The bottom part presents the thermodynamic potential density  $G_{pC}/V$  as a function of the proton density  $\rho_p$ . The straight line shows the convex envelop interpolating between the two phases A and B. This corresponds to the Maxwell construction on  $\mu_p$  as a function of  $\rho_p$  (left center). The top right part shows the convex envelop of the thermodynamic potential per particle  $G_{pC}/Z$  as a function of the inverse of the proton density  $1/\rho_p$  which is associated with a Maxwell construction for the pressure as a function of  $1/\rho_p$  (top center). The two Maxwell constructions correspond to the crossing of the  $P$ - $\mu_p$  diagram (central figure).

### C. Neutron-grand-canonical, proton-canonical ensemble

From the thermostatics point of view, using the set of state variables  $(\beta, \mu_n, \rho_p)$  corresponds to defining a neutron-grand-canonical but proton-canonical ensemble, noted as  $pC$  in the following. The associated potential per unit volume,  $G_{pC}/V = g_{pC}$ , is given by :

$$g_{pC}(\beta, \mu_n, \rho_p) = \mathcal{H} - \mu_n \rho_n - s(\mathcal{H}, \rho_n, \rho_p)/\beta$$

with  $s = S/V$  the entropy density.  $g_{pC}$  is linked by Legendre transforms both to the grand-canonical potential  $g_{GC} = -P$  (the pressure) and to the canonical potential  $f$  i.e. the free energy :

$$g_{pC} = -P + \mu_p \rho_p = f - \mu_n \rho_n.$$

Since this ensemble has only one density left, the construction of its convex envelop is a one-dimensional problem akin to the usual Maxwell construction. Numerically, we can directly perform this Maxwell construction on the function  $\mu_p(\rho_p)$  for constant  $\beta$  and  $\mu_n$ . The comparison between the results obtained using this method and the method described in the previous section using the  $\mu_p - P$  crossing point gives an estimation of our numerical error, which comes out to be less than 0.2% for all temperatures.

We can additionally remark that the above reasoning also holds if we study the  $pC$ -potential per proton leading to a Maxwell construction for the pressure  $P$  as a function  $1/\rho_p$ . Both constructions are illustrated on figure 3. The convex envelop of  $G_{pC}/V$  ( $G_{pC}/Z$ ) corresponds to an equal-area Maxwell construction on  $\mu_p(\rho_p)$  ( $P(1/\rho_p)$ ) and to the crossing point between the two phases in the  $\mu_p$  versus  $P$  graph.

It should be noticed that the introduction of a statistical ensemble in which only one density is kept, all the other ones being replaced by their associated intensive parameters, is a systematic way to study a phase transition with a one-dimensional order parameter. The only condition is that the considered density is not orthogonal to the order parameter, i.e. its value is different in the two phases. In such an ensemble, the multidimensional Gibbs construction reduces to a simple one-dimensional Maxwell construction.

### D. Variation with $\mu_n$

In order to explore the phase diagram, the method illustrated in the previous section has to be performed for various temperatures and chemical potentials. Figure 4 illustrates the  $\mu_n$  dependence for  $T = 10 \text{ MeV}$ . We can see that for a broad range of  $\mu_n$  the  $\mu_p(\rho_p)$  equations of state present a back-bending associated to an instability which must be corrected using a Maxwell construction. This defines the transition points  $\mu_p^t(\mu_n, T)$  and

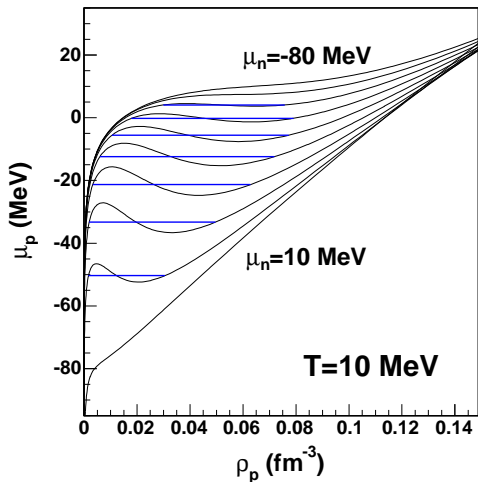


FIG. 4: Maxwell construction in the  $\mu_p$  versus  $\rho_p$  diagram for a fixed temperature  $T = 10\text{MeV}$  and regularly spaced values of  $\mu_n$  from  $-80$  to  $10\text{MeV}$ .

$P^t(\mu_n, T)$ . The ensemble of the transition points constitutes a coexistence curve at the considered temperature. This curve is limited by two critical chemical potentials,  $\mu_n^<(T)$  and  $\mu_n^>(T)$ , which in turn define the proton critical chemical potentials  $\mu_p^>(T) = \mu_p^t(\mu_n^<(T), T)$  and  $\mu_p^<(T) = \mu_p^t(\mu_n^>(T), T)$ , since  $\mu_p$  is maximum when  $\mu_n$  is minimum. The transition is observed only in a finite range of temperatures below a given temperature  $T_c$  which is nothing but the critical temperature of symmetric matter.

### E. First order phase transition

The Gibbs construction of phase coexistence leads to well defined partition sums fulfilling the thermodynamic stability requirement. The resulting pressure  $P = T \ln Z_{GC}(T, \mu_n, \mu_p)/V$  at the temperature  $T = 10\text{MeV}$  is shown in figure 5.

Along the coexistence line  $\mu_p^t(\mu_n, T)$  the pressure presents a fold i.e. the derivative perpendicular to the line is discontinuous. It is by definition a region of first-order phase transition. The coexistence line at fixed temperature is limited by two points  $(\mu_n^<(T), \mu_p^>(T))$  and  $(\mu_n^>(T), \mu_p^<(T))$ . They correspond to vertical tangents in the grand potential first derivatives  $\rho_q(\mu_n, \mu_p)$ , which are singularities in its second derivatives. Hence, the limiting points are second-order critical points, i.e points of continuous transition.

We have represented in Fig 6 the first derivative of  $\ln Z_{GC}$  in the  $\mu_n$  direction, i.e. the neutron density  $\rho_n = \partial \ln Z_{GC} / \partial \mu_n$ , which is discontinuous on the first-order line and continuous with a vertical tangent at the two critical points. Because of the exact isospin symmetry of the SLy interaction, the proton density  $\rho_p$  is symmetric to  $\rho_n$ : it is the same surface with inversion of the axes  $\mu_n$  and  $\mu_p$ .

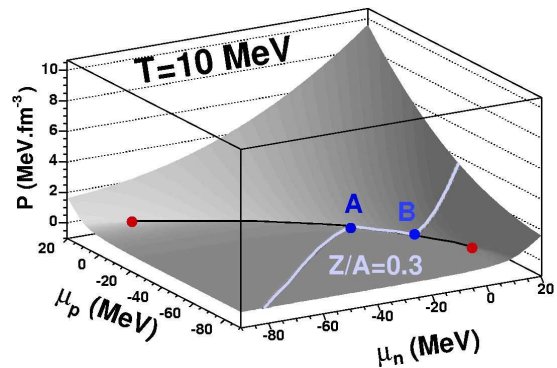


FIG. 5: Equilibrium pressure computed at a temperature  $T = 10\text{MeV}$  as a function  $\mu_n$  and  $\mu_p$  after performing a Gibbs construction for different values of  $\mu_n$ . The resulting fold line is the coexistence line ending at two critical points. The traced path corresponds to a transformation at constant proton fraction  $Z/A = 0.3$  (see Section V).

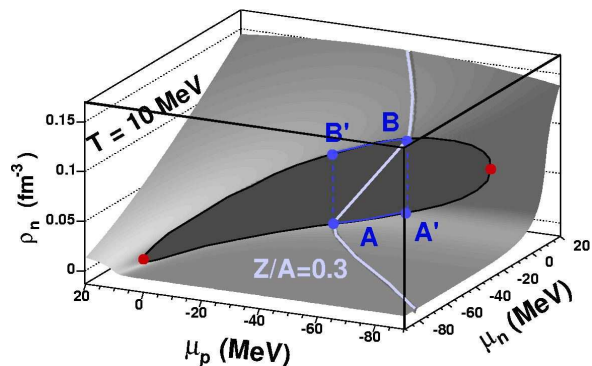


FIG. 6: First derivative of the grand-canonical partition sum,  $\rho_n = \partial p / \partial \mu_n$ , as a function of  $\mu_n$  and  $\mu_p$  at a temperature  $T = 10\text{MeV}$ . The path  $Z/A = 0.3$  is also shown.

### F. Coexistence region

The first derivatives of  $\ln Z_{GC}$  on both sides of the phase transition line define couples of points  $(\rho_n, \rho_p)$  in coexistence respectively at low (gas) and high (liquid) density. These phases merge together at the critical points. The coexistence region in the proton and neutron density space is shown on Figure 7 for a fixed temperature. The solid lines in this figure give several iso- $\mu_n$  paths. Because the construction of the concave envelop of the constrained entropy is nothing but a linear interpolation between two phases, inside the coexistence region the iso- $\mu_n$  lines are straight lines in  $(\rho_n, \rho_p)$  representation. The bottom part of the figure shows the coexistence region in the total density and proton fraction  $(\rho, Z/A)$  plane, which consists in the change of variables  $\rho = \rho_n + \rho_p$ ,  $y = Z/A = \rho_p / (\rho_n + \rho_p)$ . Because of the non linearity of the variable change, we can see that coexistence does not correspond to a straight line in

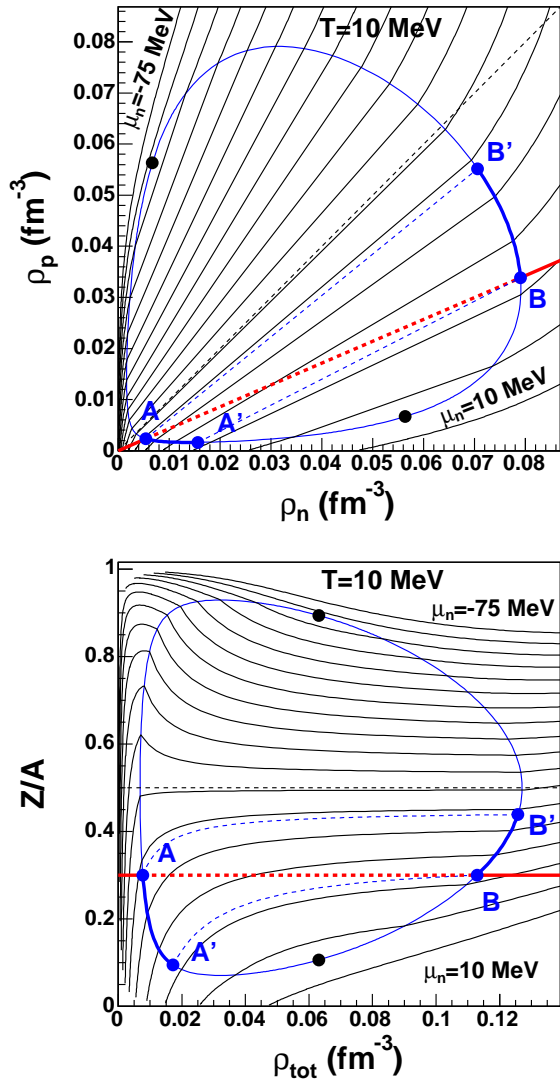


FIG. 7: Closed curves : coexistence border in the proton and neutron density plane (upper part) and total density and proton fraction plane (lower part). Black dots : critical points. Full lines : constant  $\mu_n$  paths for regularly spaced values between  $\mu_n = 10$  MeV and  $-75$  MeV. Paths  $AA'$  and  $BB'$  refer to a transformation at  $Z/A = 0.3$  (see Section V).

this representation, and the value of  $Z/A$  evolves when passing from the dense phase to the diluted phase in coexistence. The only exception is the symmetric nuclear matter case  $y = Z/A = 0.5$ .

### G. Isospin distillation

The proton fraction difference in the two phases can be appreciated from figure 8 which shows  $Z/A$  as a function of  $\mu_n$  and  $\mu_p$  for a fixed temperature  $T = 10$  MeV.  $Z/A$  being a combination of the two order parameters  $\rho_n$

and  $\rho_p$ , it also presents a discontinuity at the first order phase transition border, with the only exception of the symmetric nuclear matter point where  $Z/A = cst = 0.5$ . Correlating this plot with fig. 6, one can see that the dense phase (e.g. point B' or B) is systematically closer to isospin symmetry  $Z/A = 0.5$  than the diluted one (e.g. point A or A'). This phenomenon is known as isospin distillation [7, 20, 21].

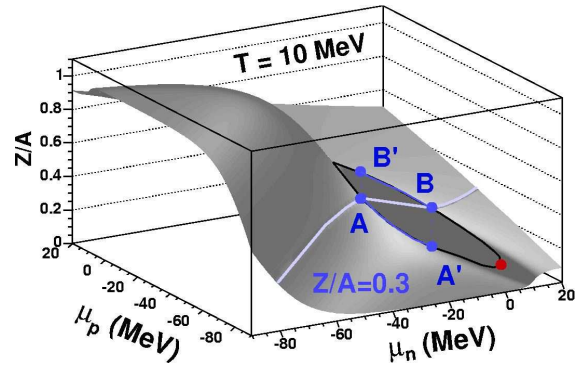


FIG. 8:  $Z/A = \rho_p/(\rho_n + \rho_p)$  as a function of  $\mu_n$  and  $\mu_p$  for a fixed temperature  $T = 10$  MeV. The path at  $Z/A = 0.3$  is also shown.

### V. TRANSFORMATION AT CONSTANT $Z/A$

In low-energy heavy-ion collisions, the proton and neutron numbers obey two independent conservation laws, implying that the proton fraction  $Z/A$  is conserved in the reaction. It is therefore of interest to consider a transformation at constant  $Z/A$  [7, 21]. In the  $(\rho_n, \rho_p)$  plane (or equivalently in the  $(\rho_{tot}, Z/A)$  representation)  $Z/A = cst$  transformations are straight lines which cross the different constant- $\mu_n$  curves. Inside the coexistence region the system with a given proton fraction is decomposed into two phases located at the intersections of the coexistence curve with the corresponding constant- $\mu_n$  curve. Since the constant- $\mu_n$  curves are not aligned on constant- $Z/A$  lines except for symmetric matter, the constant- $Z/A$  transformation does not make a transition from liquid to gas at a unique value of  $\mu_n$  but shows a continuous smooth evolution of the intensive parameters along the coexistence line.

The transformation  $Z/A = 0.3$  is given as an example by the dotted lines in Fig. 7, and the grey path in Figs. 5, 6, 8. Let us follow this transformation from the low density phase. When the system reaches the coexistence border (point A) a liquid phase appears in B' at the same value of  $\mu_n$ ,  $\mu_p$  and  $T$ . This point coincides with A in the representation of Fig. 5. We can see from Figs. 7 and 8 that the liquid fraction is closer to symmetric nuclear matter than the original system as expected from the isospin distillation phenomenon.

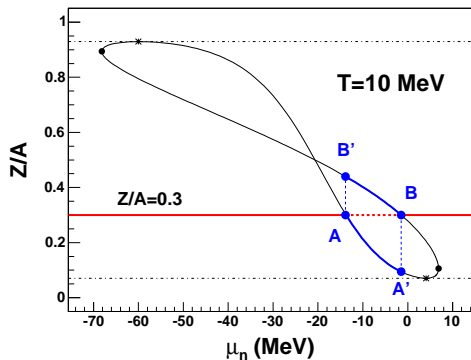


FIG. 9: Projection of the coexistence region in the  $Z/A$  versus  $\mu_n$  plane. Black dots are critical points, and stars are points of maximal asymmetry. The path at  $Z/A = 0.3$  is also shown.

Following the system inside coexistence along the line  $A - B$ , the neutron chemical potential increases. Phase separation implies that in this region the system is composed of two phases located at the coexistence boundaries and corresponding to the same value of the intensive parameters. The diluted phase goes along coexistence from  $A$  to  $A'$  while the dense phase goes on the other side of the coexistence border from  $B'$  to  $B$ . When it reaches  $B$  the gas is entirely transformed into a liquid, the phase transition is over and the  $Z/A = 0.3$  transformation corresponds to a homogenous system again.

The evolution of  $\mu_n$  during the transition can be quantitatively discussed on figure 9 which gives a projection of Fig.8 on the  $\mu_n$  axis. This figure clearly shows that a constant- $Z/A$  transformation does not cross the coexistence at a unique  $\mu_n$  value but explores a finite range of chemical potentials. The system is thus forced to follow the coexistence line in the intensive parameter space as shown in figure 5 and in Figure 10. The only exceptions are the symmetric matter and the 2 maximum asymmetries of the coexistence region for each temperature.

It is important to notice that the behavior shown in Figures 9 and 10 is the generic behavior expected when a conservation law is imposed on an order parameter[22, 23]. Indeed, the usual discontinuity of the order parameter characteristic of a first order transition is prevented by the constraint. If the system reaches coexistence, the only way to fulfill the conservation law on the order parameter is to follow the coexistence line until the conservation law becomes compatible with a homogeneous phase.

This continuous evolution by phase mixing hides the EOS discontinuity associated with the first-order phase transition. This is illustrated by the evolution of  $\mu_n$  and  $P$  as a function of the total density  $\rho_{tot}$  at  $Z/A = 0.3$  in fig. 11. Full lines are obtained after the thermodynamic potential is made convex by phase mixing, i.e. with the Gibbs construction. These functions present no plateau in the coexistence region, and the transformation looks

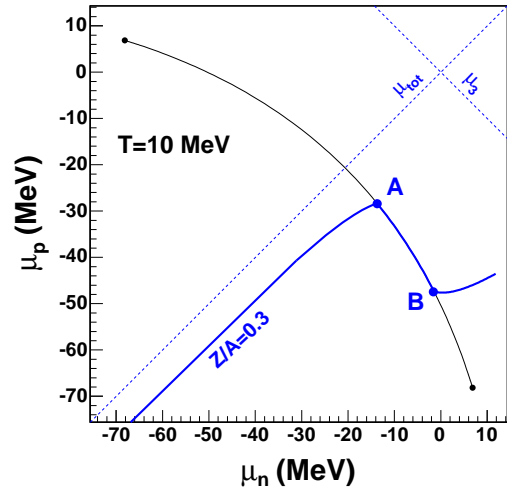


FIG. 10: Coexistence line, i.e. line of first order phase transition, in the intensive-parameter plane  $(\mu_n, \mu_p)$ . The path at  $Z/A = 0.3$  is also shown.

like a continuous transition. Yet by definition the system is going through a first-order phase transition since the first derivatives of the grand potential are discontinuous. This clearly stresses the fact that the behavior of specific transformations should not be confused with the intrinsic thermodynamic properties. In particular transformations involving a constraint on an order parameter always appear continuous even in the presence of a first order phase transition [22, 23]. The isospin degree of freedom does not change the order of the nuclear liquid-gas phase transition as claimed in different articles [7, 12]. It remains first order. Only the constant proton fraction transformations (or other transformations constraining an order parameter) mimic a continuous transition because they do not cross the coexistence line at a single point, but are forced to follow it to fulfill the conservation law.

## VI. TEMPERATURE DEPENDENCE

Until now we have presented a study at a fixed finite temperature. In this section we consider the effect of temperature on the phase diagram, from the particular case of zero temperature to the symmetric-matter critical temperature  $T_c$  above which there is no transition any more.

### A. $T = 0$ singularity

The specificity of the zero-temperature case is the possibility to reach a vanishing density with a finite chemical potential [24], while at any finite temperature a given

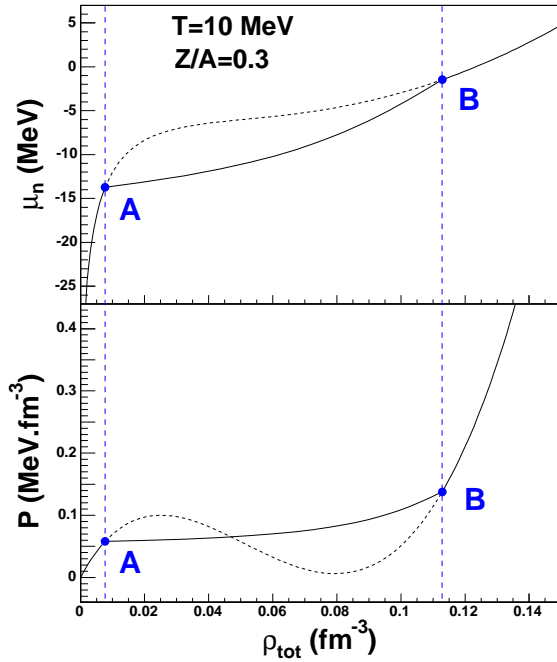


FIG. 11: Transformation at constant  $Z/A = 0.3$  in nuclear matter at  $T = 10 \text{ MeV}$ . Top :  $\mu_n(\rho_{tot})$ . Bottom :  $P(\rho_{tot})$ . Dotted lines : solution for an homogeneous system. Full lines : Gibbs construction. Points  $A$  and  $B$  give the coexistence-region borders.

density can be zero only if the associated chemical potential goes to  $-\infty$  (see eq.(5)). This is a trivial consequence of the singularity of the Dirac distribution at  $T = 0$ . In this case the associated thermodynamic potential presents at zero density an edge with a finite slope, the associated finite chemical potential. An example is given by the (free) energy as a function of total density for symmetric nuclear matter in Figure 1. Then, if the thermodynamic potential for the uniform system presents a concave intruder reaching zero density, the construction of the convex envelope does not reduce to the usual tangent construction between two points in coexistence. Indeed the interpolating plane defined by phase mixing will not be tangent to the thermodynamic potential on the zero density edge.

The coexistence region at  $T = 0$  is shown in figure 12. It can be divided into three zones corresponding to three kinds of equilibria with different conditions on the intensive parameters. In two small regions, labeled 2 in figure 12 and associated by isospin symmetry, both proton and neutron densities are finite in the gas phase. The usual bi-tangential construction can then be performed. This imposes the standard equality between all intensive parameters in the two phases  $A$  and  $B$ :  $\beta(A) = \beta(B)$ ,  $\mu_n(A) = \mu_n(B)$ ,  $\mu_p(A) = \mu_p(B)$  and  $P(A) = P(B)$ . This region is limited on one side by a critical point beyond which there is no more curvature anomaly, and on the other side by the vanishing of one of the two densi-

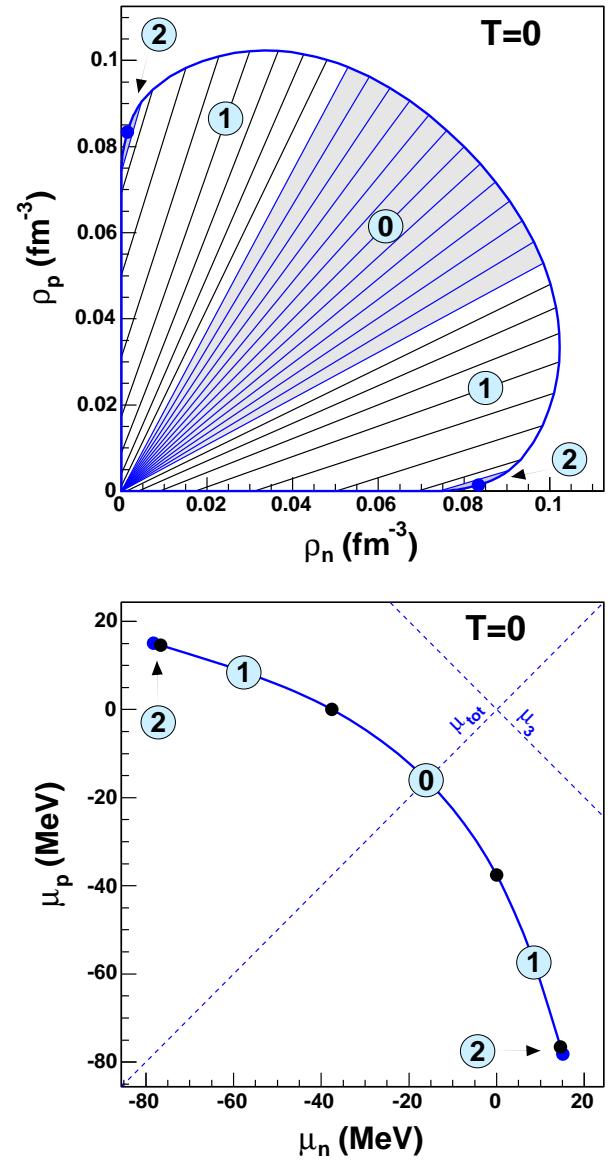


FIG. 12: Coexistence region at  $T=0$ . It is split into 3 different types of equilibria between liquid and gas (see text). Top : coexistence border (thick line) in the density plane. The straight lines relate two coexisting phases. Bottom : coexistence line in the plane of chemical potentials.

ties in the gas phase. This second case corresponds to two symmetric regions noted 1 in figure 12. There, we have equilibria for which the low density phase is on an edge  $\rho_q = 0$ , the second density being finite. For simplicity let us take the case of globally neutron-rich matter where  $\rho_p = 0$  and  $\rho_n > 0$  at the low-density coexistence edge. In this case, the convex envelop is tangent to the thermodynamic potential of the uniform system only in the dense phase. This is a mono-tangential construction. It means that phase equilibrium does not require the equality of the potential derivative in the  $\rho_p$  direction, i.e. the equality of the proton chemical potentials in the

two coexisting phases. Since the anomaly involves only the derivative in the  $\rho_p$  direction, the other equilibrium conditions characterizing the Gibbs construction are still satisfied in this region, namely the neutron chemical potential, pressure and temperature have to be the same in the two phases.

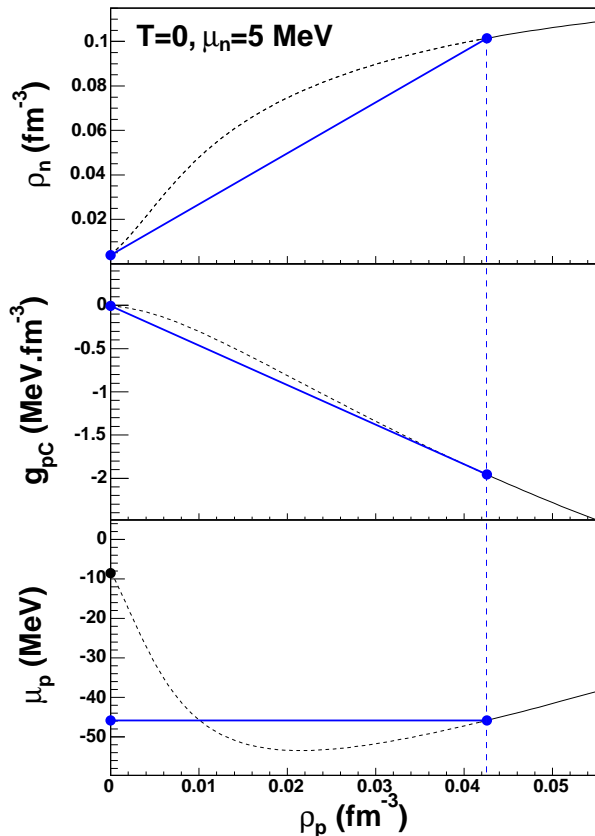


FIG. 13: Singularity at  $T = 0$ : Mono-tangential construction for a fixed neutron chemical potential  $\mu_n = 5\text{MeV}$ . Upper part: corresponding path in the density plane. It reaches the edge  $\rho_p = 0$  (with a finite  $\rho_n$ ). Middle part: thermodynamic potential density  $g_{pC}$  (see section IVC). The concave intruder is corrected by phase mixing, which corresponds here to a mono-tangential construction (straight line). Lower part:  $\mu_p$ . The mono-tangential construction on  $g_{pC}$  does not correspond to the usual Maxwell construction, that can not be performed because of the finite value of  $\mu_p$  on the edge.

Since the construction involves two points with the same  $\mu_n$  we can use the neutron-grand canonical proton-canonical potential  $G_{pC}$  (see section IVC) in order to reduce the problem to a one-dimensional case as illustrated in figure 13. This is a way to solve the problem in practice. Looking at a fixed  $\mu_n$  for which the proton density reaches its edge  $\rho_p = 0$  at zero temperature (upper part), we can see that a standard equal-area Maxwell construction is not possible in this case (lower part). However, the concave intruder in the thermodynamic potential (middle part) has to be corrected by phase mixing. Equilibrium is then given by a mono-tangential construction on  $g_{pC}$ .

Such equilibrium between a neutron gas and a two-fluid liquid leads to a discontinuous change of  $\mu_p$  in the gas. Because of the dominance of region 1 with respect to region 2 in the phase diagram, the simplification is often made in the literature [24] that phase coexistence in neutron-star matter can be modeled as the equilibrium between neutron rich nuclei and a pure neutron gas. It should however be noticed that this is possible only if the temperature is exactly zero, a finite proton fraction being associated to the gas phase at any finite temperature.

The last case, noted 0 in figure 12, corresponds to both  $\rho_p = 0$  and  $\rho_n = 0$  in the low-density phase. This case corresponds to a dense phase in equilibrium with the vacuum, i.e. at zero pressure. This region has a very simple physical interpretation. If the gas phase is given by the point  $(\rho_n, \rho_p) = (0, 0)$ , this means that the coexistence lines of zone 0 are constant  $Z/A$  lines. The coexistence border on the liquid side is the locus of zero pressure in the  $Z/A$  interval corresponding to region 0. For each value of  $Z/A$ , the liquid border is then given by the minimum of the energy per particle computed for this constant  $Z/A$ . Zone 0 corresponds then to the chemical potential interval in which a self-bound liquid can be defined.

## B. Phase diagram

In order to determine the phase diagram of nuclear matter, we establish the ensemble of points at equilibrium in the  $(\rho_n, \rho_p)$  plane for different fixed values of temperature. The result is represented in figure 14 as a function of the variables  $(\rho, Z/A)$  in order to underline the role of isospin. Since protons and neutrons play symmetric roles, the resulting curves are symmetric with respect to the axis  $Z = 0.5$ . For this reason in the following only the neutron-rich part ( $Z/A < 0.5$ ) will be discussed.

The widest coexistence region corresponds to zero temperature. Equilibrium points that belong to the edge  $\rho_p = 0$  make a line at  $Z/A = 0$ . When temperature is introduced, coexistence region concerns non-zero values of  $\rho$  and  $Z/A$ , which means that equilibrium is always between phases containing both kinds of particles.

The critical points are also reported for each temperature. They are second order transition points. They form a critical line. An interesting feature is that the critical density increases with the asymmetry while the critical temperature decreases as it can be also seen from figs. 15 and 16. This is in agreement with previous studies using different effective interactions [7, 21].

It should be stressed that on each coexistence curve at a fixed temperature the critical points do not correspond to the minimum (or maximum)  $Z/A$ . This point  $((Z/A)^{min}, \rho^{min})$  is situated at density lower than the critical point, i.e. on the gas side of coexistence. As a result, transformations can be performed at constant  $Z/A$  such that the system enters at a point of coexistence as

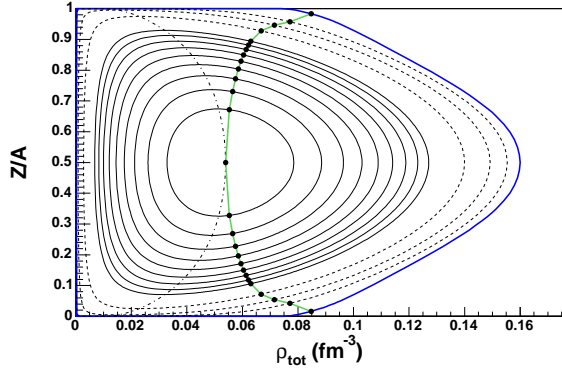


FIG. 14: Coexistence region in the  $(\rho, Z/A)$  plane at different temperatures. Thick line :  $T = 0$ . Dotted lines :  $T = 4, 6, 8 \text{ MeV}$ . Solid lines :  $T = 10, 10.5, 11, 11.5, 12, 12.5, 13, 13.5, 14 \text{ MeV}$ . Black dots : critical points at each temperature, including  $T_c = 14.54 \text{ MeV}$ . Dashed-dotted line : points of maximum asymmetry for coexistence at each temperature.

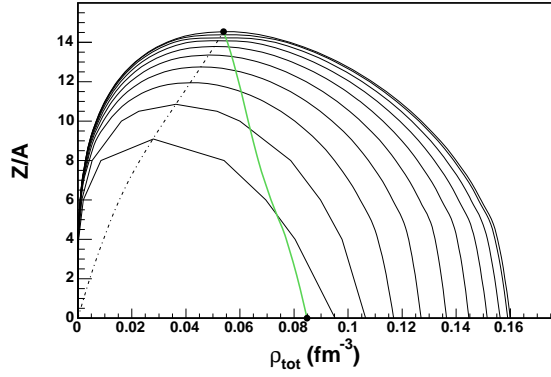


FIG. 15: Cuts of the coexistence region as a function of the total density for regularly spaced values of  $Z/A$  between 0.05 and 0.5. Thick grey line : line of critical points. Dashed-dotted line : line of maximum asymmetry.

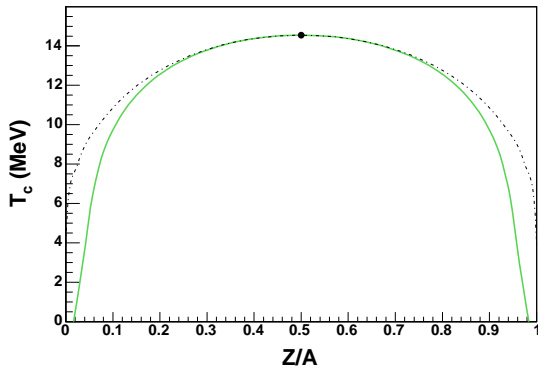


FIG. 16: Critical temperatures as a function of the system  $Z/A$  (thick grey line). The curve of maximal temperatures for coexistence is also shown (dashed-dotted line).

a gas and exits at another point still as a gas. This is the so-called retrograde transition [1]. This happens for the small region for which  $(Z/A)^{min} < Z/A < Z/A^c$ . Between those two points, there is appearance and disappearance of a liquid phase at  $(Z/A)^L > Z/A$  at equilibrium with a gas at  $(Z/A)^G < Z/A$ . For a too neutron-rich system such that  $Z/A < (Z/A)^{min}$ , there can be no phase coexistence.

As temperature grows, the coexistence region is reduced. The values of  $(Z/A)^c$  and  $(Z/A)^{min}$  become closer to the symmetry  $Z/A = 0.5$ . Densities  $\rho^c$  and  $\rho^{min}$  follow opposite evolutions:  $\rho^{min}$  grows with temperature, while  $\rho^c$  diminishes. The coexistence region disappears at the critical temperature  $T^c$ , for which only symmetric matter presents a second order transition point. Critical and minimum  $Z/A$  lines join at this ultimate critical point.

It is also interesting to look at the coexistence zone as a function of  $Z/A$  (see Figures 15, 16). We can see that the dependence of the critical temperature (as well as the maximal temperature) on  $Z/A$  is weak. Only for very high values of asymmetry the difference between the two temperatures for a fixed  $Z/A$  can be several MeV. This is another way to visualize the retrograde transition, meaning that we can have saturated vapor at supercritical temperatures.

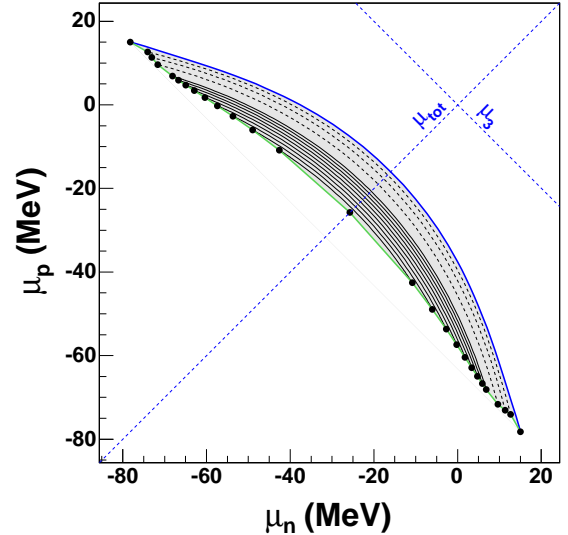


FIG. 17: Phase diagram in  $(\mu_n, \mu_p)$  for different values of  $T$ . Thick line :  $T = 0$ . Dotted lines :  $T = 4, 6, 8 \text{ MeV}$ . Solid lines :  $T = 10, 10.5, 11, 11.5, 12, 12.5, 13, 13.5, 14 \text{ MeV}$ . Black dots : critical points at each temperature, including  $T_c = 14.54 \text{ MeV}$ .

Finally, it is interesting to look at the coexistence manifold in the  $(\beta, \mu_n, \mu_p)$  space, as shown in Figure 17. One can see that the coexistence is almost perpendicular to the  $\mu_3 = 0$  axis, stressing the fact that the nuclear liquid-gas phase transition is dominated by its isoscalar component [25, 26].

## VII. CRITICAL BEHAVIOR

Let us now study in more details the critical behavior of the system. Conversely to the usual single-fluid liquid-gas phase transition which presents a unique critical point, a two-fluid system is critical along a line in the  $(\beta, \mu_n, \mu_p)$  intensive-parameter space. The critical points are obtained for each temperature below the symmetric-matter critical temperature determining the  $\mu_n$  value for which the two phases with the same tangent plane merge together. To evaluate this point, we have used both the Maxwell construction in the neutron-grand-canonical proton-canonical ensemble (see section IVC) and the existence of a crossing point in the  $P$  versus  $\mu_p$  curve at constant  $T, \mu_n$  (see section IVB). The critical points also correspond to the disappearance of a concave intruder in the uniform system free energy. This disappearance of the spinodal region provides an independent way to evaluate the location of the critical line: we can represent as a function of  $\mu_n$  the lower value of the free energy curvature in the  $(\rho_n, \rho_p)$  plane. The resulting curve crosses the horizontal axis at the critical value of  $\mu_n$ . Below the symmetric matter critical point  $T_c$ , these methods lead to the definition of two symmetric critical lines, one for neutron-rich systems ( $\mu_n = \mu_n^>(T)$ ,  $\mu_p = \mu_p^<(T)$ ) and the other for the opposite isospin ( $\mu_p = \mu_p^>(T)$ ,  $\mu_n = \mu_n^<(T)$ ).

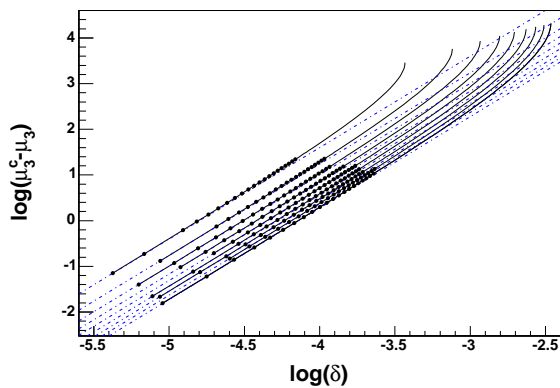


FIG. 18: Solid lines with points : evolution of  $\mu_3 - \mu_{3c}$  as a function of  $\delta$  (see text) near the critical point for different temperatures :  $T = 10, 10.5, 11, 11.5, 12, 12.5, 13, 13.5, 14 MeV$ . Straight dashed-dotted lines : power laws with critical exponent  $\beta_\beta = 2$ .

At the approach of the critical point, the distance in the space of observables between the two phases ( $A$  and  $B$ ) in equilibrium, i.e. the order parameter, goes to zero as a power of the distance to the critical point in the intensive-variable space. The resulting power law is characterized by the critical exponent  $\beta$ . In order to study this behavior for nuclear matter in the  $(\rho_n, \rho_p)$  plane, we consider a distance  $\delta = \sqrt{(\rho_n^B - \rho_n^A)^2 + (\rho_p^B - \rho_p^A)^2}$ . In a two-fluid system the behavior of this distance can be

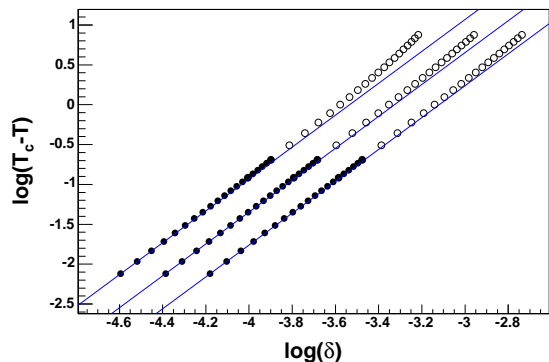


FIG. 19: Points : evolution of  $T - T_c$  as a function of  $\delta$  (see text) near the critical point for different  $\mu_n$ :  $\mu_n = \mu_q^<(T_c)$ ,  $\mu_q^<(T = 12 MeV)$ ,  $\mu_q^<(T = 10 MeV)$ . Straight lines: power laws with critical exponent  $\beta_{\mu_n} = 2$ .

studied in two ways.

First, for a fixed temperature  $T = \beta^{-1}$ ,  $\delta$  is expected to depend on the chemical potentials as :

$$\delta_\beta(\mu_q) \propto (\mu_q^c - \mu_q)^{1/\beta_\beta} \quad (8)$$

where  $\beta_\beta$  is the critical exponent at a fixed temperature and  $\mu_q^c$  the critical value of  $\mu_q$  for the considered temperature. Since  $\mu_n$  and  $\mu_p$  are constrained to be on the coexistence line, the above relation is independent of the chemical potential selected to perform the study. For symmetry reasons we have introduced the isoscalar  $\mu = \mu_n + \mu_p$  and the isovector  $\mu_3 = \mu_n - \mu_p$  chemical potentials. Since the dependence on  $\mu$  is negligible (see Figure 17) we have focused our study on the evolution of  $\delta$  with  $\mu_3$ . The results are presented in Figure 18. We can observe that our results perfectly follow the expected critical behavior with the mean field value  $\beta_\beta = 2$ .

For a fixed value of  $\mu_q$ , the distance  $\delta_{\mu_q}$  goes to zero as the temperature tends to the critical one  $\beta^c$ . The power law should be :

$$\delta_{\mu_q}(\beta) \propto (\beta^c - \beta^q)^{1/\beta_{\mu_q}} \quad (9)$$

where  $\beta_{\mu_q}$  is the critical exponent at a fixed  $\mu_q$ . Again since the temperature  $\beta$  and the chemical potential  $\mu_q$  in coexistence are related by a Clapeyron-like relation, the above study leads to the same critical behavior if studied as a function of  $\mu_{q'}$  with  $q' \neq q$ , instead of  $\beta$ . In figure 19 we present the evolution with temperature for different chemical potentials. This graph shows that our results fulfil the mean field scaling  $\beta_{\mu_q} = 2$ .

## VIII. CONCLUSION

In this paper, based on a mean-field analysis of nuclear matter with a realistic Skyrme SLy230a effective interac-

tion, we have established that nuclear matter presents a first-order phase transition even when the isospin degree of freedom is explicitly accounted for. This results from the existence of a spinodal region, which is a region where the free energy of a homogeneous system is concave. In the case of infinite systems, such curvature anomaly is corrected by constructing the convex envelope. This is a tangent construction that links couples of points in the space of observables with the same values for the intensive parameters. It corresponds to points of discontinuous first derivatives for the grand-canonical potential of the system in the space of Lagrange intensive parameters, along a coexistence manifold limited by a critical line. Except on this limit which corresponds to a second-order phase transition, the slope discontinuity demonstrates that the system is undergoing a first-order phase transition. For fixed values of temperature (below the symmetric-matter critical one), coexistence lines are obtained in the chemical-potential plane. They are limited by critical points that correspond to proton fractions depending on the temperature. As lower temperatures are considered, more asymmetric nuclear matter can be

involved in a first-order phase transition.

As for the study of critical behaviors, we have found that all the numerical data can be fitted by power laws with critical exponents equal to 2, which is consistent with generic mean field predictions [27]. Calculations beyond the mean field are needed to obtain a result which could be characteristic of a given universality class. Looking at the isospin content of the phases, we show that the proton fraction is discontinuous at the phase transition except at the critical points and for symmetric matter. In asymmetric nuclear matter, the proton fraction can be used as an order parameter. When the transition occurs the liquid gets closer to symmetry while the gas is enriched in the more abundant species. This is the well known isospin fractionation. This has a strong influence on the constant proton fraction transformations, since in order to fulfill the imposed conservation on an order parameter the transformation is forced to follow the coexistence line instead of crossing it. This hides the slope discontinuity characteristic of a first-order phase transition, the transformation appearing as continuous.

- 
- [1] K.Huang, *Statistical Mechanics*, Wiley 1963
  - [2] J.E.Finn et al., *Phys. Rev. Lett* 49 (1982) 1321
  - [3] G.Bertsch, P.J.Siemens, *Phys. Lett. B* 126 (1983)
  - [4] C.B.Das et al, *Phys. Rep.* 406 (2005) 1
  - [5] J.M.Lattimer and M.Prakash, *Phys. Rep.* 333 (2000) 121
  - [6] N.K.Glendenning, *Phys. Rep.* 342 (2001) 393.
  - [7] H.Muller and B.Serot, *Phys. Rev. C*52 (1995) 2072.
  - [8] C.B.Das et al, *Phys. Rev. C*67 (2003) 064607;
  - [9] W.L.Qian, S.R.Keng, *Journ. Phys. G* (2003) 1023
  - [10] T.Sil et al., *Phys. Rev. C*69 (2004) 14602
  - [11] B.K.Srivastava et al., *Phys. Rev. C*65 (2002) 054617
  - [12] J.M.Carmona et al., *Nucl. Phys. A*643 (1998) 115
  - [13] E.Chabanat et al., *Nuclear Physics A*627 (1997) 710-746.
  - [14] R. Balian, *From Microphysics to Macrophysics*, Springer Verlag, 1982.
  - [15] M.Barranco, J.R.Buchler, *Phys. Rev. C*24 (1981) 1191
  - [16] J.M.Lattimer, C.J.Pethick, D.G.Ravenhall, D.Q.Lamb, *Nucl. Phys. A*432 (1985) 646
  - [17] S.Shlomo, V.M.Kolomietz, *Rep. Prog. Phys.* 68 (2005) 1
  - [18] F.Douchin, P.Haensel and J.Meyer, *Nucl. Phys. A*665 (2000) 419
  - [19] D.Vautherin, *Adv. Nucl. Phys.* 22 (1996) 123.
  - [20] V.Baran et al, *Nucl.Phys. A*632 (1998) 287.
  - [21] B.A.Li, C.M.Ko and W.Bauer, *Int. Journ. Mod. Phys. E*7 (1998) 147
  - [22] Ph.Chomaz and F.Gulminelli, in 'Dynamics and Thermodynamics of systems with long range interactions', *Lecture Notes in Physics* vol.602, Springer (2002)
  - [23] F. Gulminelli et al, *Phys.Rev.E*68 (2003) 026120.
  - [24] C.J.Pethick, D.G.Ravenhall, C.P.Lorenz, *Nucl. Phys. A*584 (1995) 675.
  - [25] J.Margueron, Ph. Chomaz, *Phys. Rev. C*67 (2003) 041602;
  - [26] V.Baran et al, *Phys. Rep.* 410 (2005)335.
  - [27] H.E.Stanley, *Introduction to phase transitions and critical phenomena*, Oxford University press, 1971.